Taylor & Francis
Taylor & Francis Group

Vibrational Fingerprints of LiNbO$_3$-LiTaO$_3$ Mixed Crystals

S. SANNA,[1] A. RIEFER,[1] S. NEUFELD,[1] W. G. SCHMIDT,[1]
G. BERTH,[2] M. RÜSING,[2] A. WIDHALM,[2] AND A. ZRENNER[1]

[1]Lehrstuhl für Theoretische Physik, Universität Paderborn, Warburgerstraße 100, 33098 Paderborn, Germany
[2]Center for Optoelectronics and Photonics (CeOPP) and Department Physik, Universität Paderborn, Warburgerstraße 100, 33098 Paderborn, Germany

Atomistic simulations in the framework of the density functional theory have been used to model morphologic and vibrational properties of lithium niobate–lithium tantalate mixed crystals as a function of the [Nb]/[Ta] ratio. Structural parameters such as the crystal volume and the lattice parameters a *and* c *vary roughly linearly from LiTaO$_3$ to LiNbO$_3$, showing only minor deviations from the Vegard behavior. Our* ab initio *calculations demonstrate that the TO$_1$, TO$_2$ and TO$_4$ vibrational modes become harder with increasing Nb concentration. TO$_3$ becomes softer with increasing Nb content, instead. Furthermore, the investigated zone center* A$_1$*-TO phonon modes are characterized by a pronounced stoichiometry dependence. Frequency shifts as large as 30 cm^{-1} are expected as the [Nb]/[Ta] ratio grows from 0 to 1. Therefore, spectroscopic techniques sensitive to the* A$_1$ *modes (such as Raman spectroscopy), can be employed for a direct and non-destructive determination of the crystal composition.*

Keywords Ferroelectrics; vibrational properties; LiNbO$_3$; LiTaO$_3$; mixed crystals

I. Introduction

Both lithium niobate (LiNbO$_3$, LN) and lithium tantalate (LiTaO$_3$, LT) are optical materials widely used for a variety of applications ranging from optical modulators over photo-refractive and acoustic devices to frequency doubling. Thereby mainly the piezo- and ferroelectric properties of the materials are exploited. In particular, LN is probably the most important electro-optic material, while LT is mainly employed as a LN replacement for shorter wavelength applications [1]. Both materials crystallize within the *R*3*c* space group and share several common physical and chemical properties. Commercially available crystals are usually Czochralsky grown and lithium deficient ([Li] /[Nb], [Ta] < 1), which results in a highly defective structure of congruent composition. Above the Curie temperature (607°C for LT and 1142°C for LN) a phase transition to a high-symmetry paraelectric phase (space group *R*$\bar{3}$*c*) occurs.

Mixed crystals have recently attracted the attention of the scientific community, as they offer the possibility to tune the physical properties by varying the composition. Lithium niobate-tantalate (LNT, LiNb$_{1-x}$Ta$_x$O$_3$) is one of the simplest ferroelectric mixed crystals,

which shows quite unusual physical properties. In particular, the existence of a composition with zero birefringence at room temperature is unique in ferroelectric nonlinear-optical materials. Indeed, within this composition the crystal is optical isotropic and yet electrically polar [2, 3].

Despite the huge potential in electro-optic and acousto-optic devices and the extensive use of the end-compounds LN and LT, relatively little is known about the mixed crystals [4]. This is mainly due to the difficulty to grow compositionally homogeneous crystals with traditional methods such as the Czochralski growth from a lithium rich melt. In fact, despite the isomorphism of the end compounds and the similar radii and valence of Ta and Nb, the large separation of the solid-liquid lines in the LN-LT phase diagram makes the crystal growth across the composition range a technically demanding task. However, the growth of homogeneous crystals by several techniques has been demonstrated recently [2].

In this contribution, we investigate the structural and vibrational properties of ferro-electric $LiNb_{1-x}Ta_xO_3$ over the whole composition range by *first-principles* simulations. The relevance of the paraelectric phase in technological applications is extremely limited by the high Curie temperature. Therefore it will not be investigated in this work. To our knowledge, our work represents the first theoretical modeling of LNT mixed crystals.

II. Methodology

Total energy density functional calculations have been performed within the PW91 formulation of the generalized gradient approximation (GGA) [5] as implemented in the VASP simulation package [6]. PAW potentials [7] with projectors up to $l = 3$ for Nb, Ta and $l = 2$ for Li, O have been used for the calculations. The electronic wave functions are expanded into plane waves up to a kinetic energy of 400 eV. Our work is therefore on the same footing of previous calculations on LN bulk crystals [8]. This approach yields lattice parameters *a* and *c* as well as internal parameter *z*, *u*, and *w* for the end compounds $LiNbO_3$ and $LiTaO_3$ within 1–2% of the experimental values. Rhombohedral supercells containing 20 atoms (i.e. a $2 \times 1 \times 1$ repetition of the LN primitive cell) were used in order to model Ta concentrations of 0%, 25%, 50%, 75% and 100%. The influence of the cation distribution in the mixed crystals on energetics, geometries and phonon modes is accounted for by averaging over the different configurations realizable with our supercells. Thus, our calculations refer to stoichiometric, compositionally homogeneous crystals: the investigation of the commonly used congruent materials is beyond the goals of this work. Also, the influence of local stoichiometry fluctuations or intrinsic defects is not investigated here. A Γ-centered $8 \times 8 \times 8$ k-point mesh was used to carry out the integration in the Brillouin zone. The atomic positions were allowed to relax until the Hellman-Feynman forces acting on each atom were lower than 10 meV/Å. The phonon modes and frequencies are calculated using the frozen-phonon approach [9]. This approach does not include the long-range electric fields that accompany longitudinal phonons. For this reason, we limit ourselves to the investigation of transverse modes.

III. Results

In the first step the equilibrium lattice parameters are calculated for all the investigated concentrations. Thereby, atomic positions and primitive vectors are optimized at fixed volume for a set of 15 different volumes in the range of ±5% of the measured LN volume. The total energy as a function of the cell volume is then fitted to the Murnaghan state
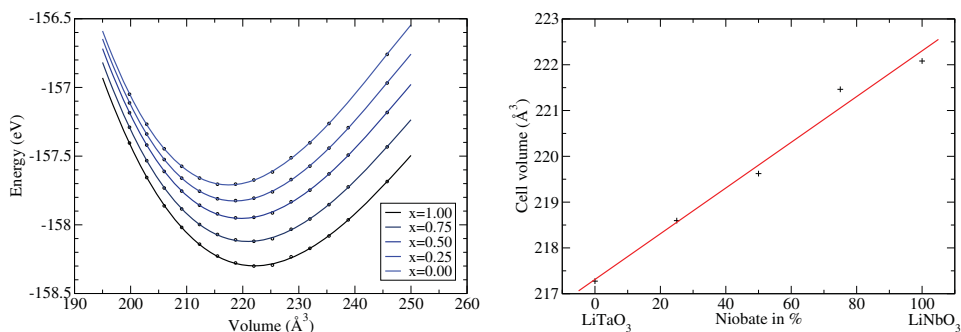
Figure 1. Lattice parameters of the LiNb$_x$Ta$_{1-x}$O$_3$ mixed crystals: Murnaghan fit of the calculated data (left hand side) and calcuated unit cell volume as a function of the Nb concentration (right hand side). The volume grows roughly linearly from LiTaO$_3$ to LiNbO$_3$.

equation [10]

$$E(V) = V_0 \frac{B}{B'} \left[\frac{1}{B'-1} \left(\frac{V_0}{V} \right)^{B'-1} + \frac{V}{V_0} \right] + const \tag{1}$$

where B is the bulk modulus, B' its first derivative and V_0 the equilibrium volume. The calculated point are perfectly fitted by the state equation as shown in Fig. 1 (left hand side). A further calculation is then performed at the Murnaghan minimum in order to find the equilibrium total energy and structural parameters for each composition. The Murnaghan state equation also yields information about the crystal response to external pressure (the bulk moduli B and B'), which however, is not discussed in this work. As shown in Fig. 1 (right hand side), the supercell volume grows almost linearly from LT to LN (Vegard behavior), while minor deviations from the linearity of the lattice parameters a and c are observed. This is in agreement with recent X-ray diffraction measurements [2] and older experimental data [11]. The volume difference of about 2% between LiTaO$_3$ and LiNbO$_3$ reflects the differences in atomic size between Ta and Nb [12].

In the second step the phonon modes are modeled within the frozen-phonon approach at the calculated equilibrium geometries. The Γ-TO modes of crystals belonging to the *R3c* space group (such as the end compounds LN and LT) can be classified on the basis of their symmetry into *A* (four A_1, five A_2) and *E* (nine) modes. The A_2 modes are not Raman active and will not be discussed in this work. An analysis of the phonon eigenvectors allows to classify the calculated modes as A_1 (if the mode preserves the full crystal symmetry), as A_2 (symmetry preserved, the ions of the same type vibrate in antiphase) and E modes (the crystal symmetry is not preserved, the mode is doubly degenerate). The eigenvectors of the four A_1 modes investigated in this work are represented in Fig. 2 (labeled by TO$_1$ to TO$_4$). The plotted displacement patterns lead to a change of the crystal polarization, which explains why the A_1 modes are both Raman and Infrared visible.

Within the DFT calculations, the LN A_1 modes are found at 235, 254, 323, and 609 cm^{-1}, and the corresponding LN modes at 200, 242, 348, and 577 cm^{-1}. Within deviations of at most 30, but typically about 10 cm^{-1} (which is mainly due to anharmonicity effects), the calculated frequencies match the experimental findings, both for LN and LT [14–16]. The accuracy of our calculations is thus comparable to earlier frozen-phonon calculations [9, 13].
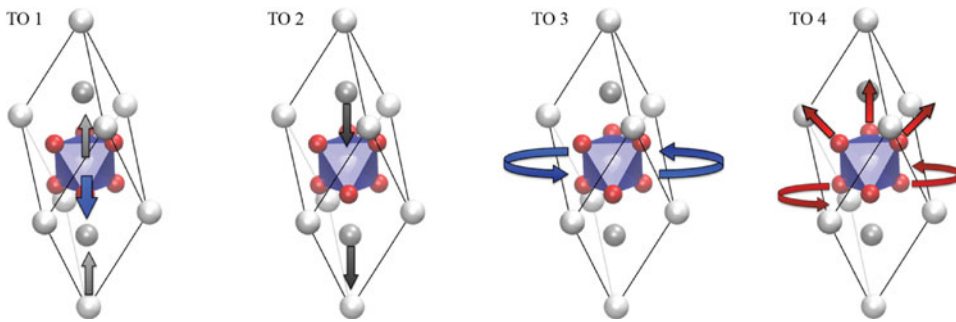
Figure 2. Eingenvectors of the four vibrational transversal branches (TO1 to TO4) of LiNbO$_3$ and LiTaO$_3$. Arrows represent schematically the displacement patterns (see text for further details).

As shown in Fig. 2, TO$_1$ is essentially a *z*-vibration, with the Nb,Ta ions vibrating in antiphase with the oxygen octahedra. TO$_2$ is a *z*-vibration as well, in which only the Li ions are displaced from the equilibrium positions. TO$_3$ and TO$_4$ essentially involve the oxygen octahedra and the ionic displacements take place in the *xy*-plane. While TO$_3$ consists of an almost rigid rotation of the whole octahedra, in TO$_4$ the displacement pattern is more complex. The ions in one oxygen plane rotate about the trigonal axis as in TO$_3$, while the ions of the other plane show a typical breathing movement. The oxygen octahedra are thus distorted and the mode is occupied at considerably higher energies than TO$_3$. A more detailed description of the TO-mode eigenvectors can be found, among others in [13]. The description of the displacement patterns of the non symmetry-conserving *E* modes is beyond the goals of this study.

The frequencies of the *A$_1$* modes for the mixed crystals are compiled in Table 1 and plotted as a function of the Ta concentration in Fig. 3. As the Ta ions (atomic mass 180.95 amu) are much more massive than the Nb ions (atomic mass 92.906 amu), one would expect much harder phonon modes for LN than for LT. Furthermore, depending on the participation of Nb,Ta to the different modes (represented in Fig. 2), the frequency dependence of the four phonons is expected to be different. Indeed, while TO$_1$ (displacement of the Nb,Ta ions with respect to the oxygen octahedra) shows a strong composition dependence, TO$_2$ (involving solely Li ions) is only slightly blue-shifted from LT to LN. While TO$_1$, TO$_2$ and TO$_4$ become harder with increasing Nb concentration, TO$_3$ softens continuously from LiTaO$_3$

Table 1

Zone center phonon frequencies (in cm^{-1}) calculated for several LiNb$_{1-x}$Ta$_x$O$_3$ stoichiometries. The TO$_3$ mode becomes blue-shifts with increasing Ta concentration, while the other become softer

Mode	Composition				
	LN	LN$_{.75}$T$_{.25}$	LN$_{.50}$T$_{.50}$	LN$_{.25}$T$_{.75}$	LT
TO$_1$	235	229	214	208	200
TO$_2$	254	244	241	242	242
TO$_3$	323	327	335	342	348
TO$_4$	609	598	588	582	577
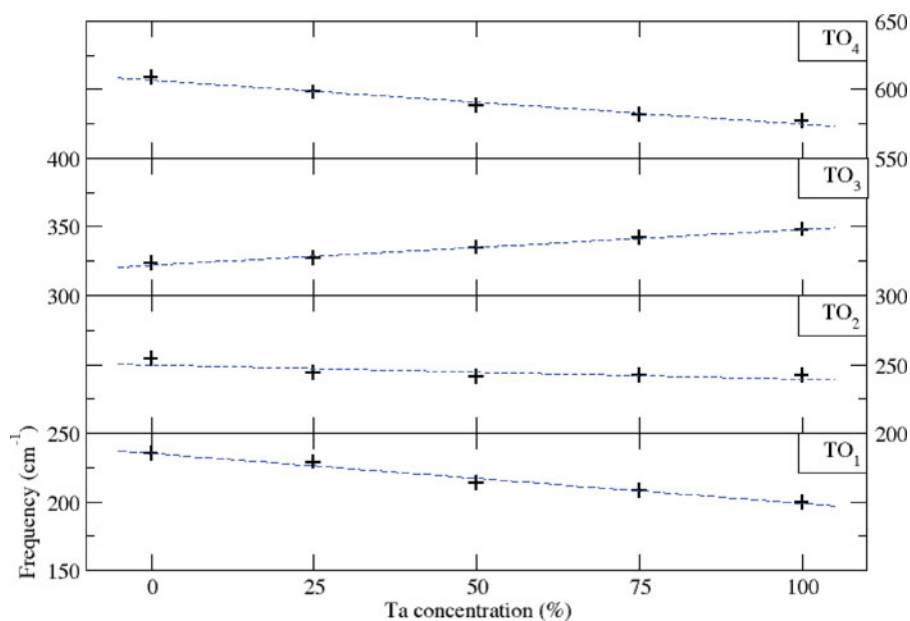
Figure 3. Composition dependence of the four A_1 TO-modes in LiNb$_{1-x}$Ta$_x$O$_3$ mixed crystals. The dashed line is the linear fit of the calculated points. (Color figure available online).

to LiNbO$_3$. This behavior cannot be simply explained by the different atomic mass, but is related to the different binding of the Ti and Nb ions with the oxygen sublattice. Indeed, it has been previously attributed by Caciuc and Postnikov [15] to a comparatively harder oxygen rotation in LiTaO$_3$. The TO$_3$ mode shows, however, a less pronounced dependence on the composition with respect to other TO phonons. Because of their pronounced composition dependency, the TO modes are true fingerprints of the crystal stoichiometry. In particular TO$_1$ and TO$_4$ can be used to identify the crystal composition by direct and non-destructive Raman measurements.

IV. Conclusions

The morphologic and vibrational properties of LiNb$_{1-x}$Ta$_x$O$_3$ mixed crystals have been modeled within the density functional theory. The crystal volume grows roughly linearly from LiTaO$_3$ to LiNbO$_3$. The lattice parameters a and c of the rhombohedral structure exhibit only small deviations from a linear dependence on the composition. The zone center phonon modes (TO Γ-modes) have been calculated with the frozen phonon approach. Our models predict a pronounced stoichiometry dependence of several phonons, in particular the TO$_1$ and TO$_4$ transversal optic modes show a frequency shift as large as 30 cm^{-1} as the Nb concentration grows from 0 to 1. The stoichiometry dependence has been explained, depending on the involved atomic species either by the Nb-Ta atomic mass difference or by the different Nb-O and Ta-O atomic bond. According to our calculation, these phonons are true fingerprints of the crystal stoichiometry. Therefore Raman spectroscopy measurements can be used to identify the crystal composition in a direct and non-destructive manner.

Acknowledgments

References

1. R. S. Weis and T. K. Gaylord, Lithium-niobate - summary of physical-properties and crystal-structure. *Appl. Phys. A*, vol. **37**, pp. 191–203 (March 1985).

2. A. Bartasyte, A. M. Glazer, F. Wondre, D. Prabhakaran, P. A. Thomas, S. Huband, D. S. Keebl, and S. Margueron, Growth of $LiNb_{1-x}Ta_xO_3$ solid solution crystals. *Mat. Chem. and Phys.*, vol. **134**, pp. 728–735 (June 2012).

3. I. G. Wood, P. Daniels, R. H. Brown, and A. M, Glaze, Optical bire-fringence study of the ferroelectric phase transition in lithium niobate tantalate mixed crystals: $LiNb_{1-x}Ta_xO_3$. *J. Phys.: Condens. Matter*, vol. **20**, pp. 235237–235242 (May 2008).

4. D. Xue, K. Betzler, and H. Hesse, Dielectric properties of lithium niobate–tantalate crystals, *Sol. Stat. Comm.*, vol. **115**, pp. 581–585 (Aug. 2000).

5. J. P. Perdew and Y. Wang, Accurate and simple density functional for the electronic exchange energy: Generalized gradient approximation, *Phys. Rev. B*, vol. **33**, pp. 8800–8802 (June 1986).

6. G. Kresse and J. Furthmüller, Efficient iterative schemes for ab initio total-energy calculations using a plane-wave basis set. *Phys. Rev. B*, vol. **54**, pp. 11169–11186 (Oct. 1996).

7. P. E. Blöchl, Projector augmented-wave method, *Phys. Rev. B*, vol. **50**, pp. 17953–17979 (Dec. 1994).

8. W.G. Schmidt, M. Albrecht, S. Wippermann, S. Blankenburg, E. Rauls, F. Fuchs, C. Rödl, J. Furthmüller, and A. Hermann, $LiNbO_3$ ground- and excited-state properties from first-principles calculations. *Phys. Rev. B*, vol. **77**, pp. 035106–035112 (Jan. 2008).

9. W. G. Schmidt, F. Bechstedt, and G. P. Srivastava, III-V(110) surface dynamics from an ab initio frozen-phonon approach, *Phys. Rev. B*, vol. **52**, pp. 2001–2007 (July 1995).

10. F. D. Murnaghan, The compressibility of media under extreme pressures, *Proc. Nat. Acad. Sci. USA* vol. **30**, pp. 244–247 (Sept. 1944).

11. F. Shimura, Y. Fujino, Crystal growth and fundamental properties of $LiNb_{1-y}Ta_yO_3$, *J. Cryst. Growth*, vol. **38**, pp. 293–301 (June 1977), and references therein.

12. E. Clementi, D. L. Raimondi, and W. P. Reinhardt, Atomic Screening Constants from SCF Functions, *J. Chem. Phys.*, vol. **38**, pp. 2686–2689 (June 1963).

13. S. Sanna, G. Berth, W. Hahn, A. Widhalm, A. Zrenner and W. G. Schmidt, Vibrational properties of the $LiNbO_3$ z-surfaces, IEEE Transactions on ultrasonics, ferroelectrics and frequency control, vol. **58**, pp. 1751–1756 (September 2011).

14. C. Rapitis, Assigment and temperature dependence of the Raman modes of $LiTaO_3$ studied over the ferroelectric and paraelectric phases, *Phys. Rev. B*, vol. **38**, pp. 10007–10019 (Nov. 1988).

15. V. Caciuc and A.V. Postnikov, Ab initio zone center phonons in $LiTaO_3$: Comparison to $LiNbO_3$, *Phys. Rev. B*, vol. **64**, pp. 224403–224409 (Nov. 2001).

16. A. Ridah, M. D. Fontana, and P. Bourson, Temperature dependence of the Raman modes in $LiNbO_3$ and mechanism of the phase transition, *Phys. Rev. B*, vol. **56**, pp. 5967–5973 (Sep. 1997).